

National Report of Greece to EUREF 2015

M.Gianniou, E. Mitropoulou, D. Mastoris
National Cadastre and Mapping Agency S.A.
Mesogion Ave. 288, 15562 Athens, Greece

1. Introduction

During the last months the main activities of the National Cadastre and Mapping Agency of Greece (NCMA S.A.) related to EUREF include:

- Monitoring of the ionospheric activity over Greece
- Study of reference station displacements as a result of the 2014 North Aegean Sea earthquake.

This national report describes the aforementioned activities.

2. Monitoring of the ionospheric activity over Greece

During 2011 and 2012 intense ionospheric activity seriously affected the performance of RTK measurements in Greece, mainly in the southern part of the country. RTK-users had often needed longer times to obtain fixed solution than in the years before. Sometimes, initialization could hardly be achieved (Gianniou and Mitropoulou, 2012). On this occasion and knowing that the maximum of the 24th Solar Cycle was about to come, NCMA S.A. started in 2012 to monitor the ionospheric index I95 (Wanninger, 1999) in order to support the HEPOS users in the most efficient way (Gianniou and Mastoris, 2013). The time-series of I95 of HEPOS describes quite well the ionospheric activity over Greece in the years around the maximum of the 24th Solar Cycle. Fig. 1 shows the daily maximum of I95 for Crete and for the rest of the HEPOS network (mainland and islands) for the time period January 2010 to May 2015. As it can be seen, the maximum of the 24th Solar Cycle did not take place in 2003, as it was initially expected. Actually, the 24th Solar Cycle proved to be double-peaked. Furthermore, the second peak was higher than the first one. These facts had already been observed in 2014 examining the time-series from January 2010 to May 2014 (Gianniou et al., 2014). At the time of writing (May 2015) the sunspot number is already decreasing. Thus, the extension of the time-series to May 2015 describes better the ionospheric activity during the maximum of the 24th Solar Cycle.

A more representative overview of the ionospheric activity can be obtained using mean daily I95 values, instead of daily maximum values. So, starting from 1.1.2010 a mean I95 value (mean daily) was computed for each day from the 24 hourly values available in HEPOS for every day. Fig. 2 shows the mean daily I95 values (smoothed using a moving average filter with a span of 7 days). The two peaks of the 24th Solar Cycle (around November 2011 and March 2014) can clearly be seen, with the second one being higher.

In order to compare the I95 index (mean daily values) with other measures of the ionospheric/solar activity time-series of the Total Electron Content (TEC) and the sunspot number were examined. Fig. 3 shows the TEC values obtained from the Global Ionospheric Maps (GIM) produced by CODE (Centre for Orbit Determination in Europe). More specifically, the TEC values of Fig. 3 refer to the point with coordinates $\varphi=37.5^\circ$, $\lambda=25^\circ$ and to 12:00 UTC (TEC values are smoothed using a moving average filter with a span of 7 days). This point is representative for the main part of the HEPOS network (mainland and islands) and so, the time-series of Fig. 3 is comparable to the blue line of Fig. 2. As it was expected, the time-series of I95 and TEC are highly correlated. Of course, there is not a 100% correlation as the vertical TEC refers to the charge of the

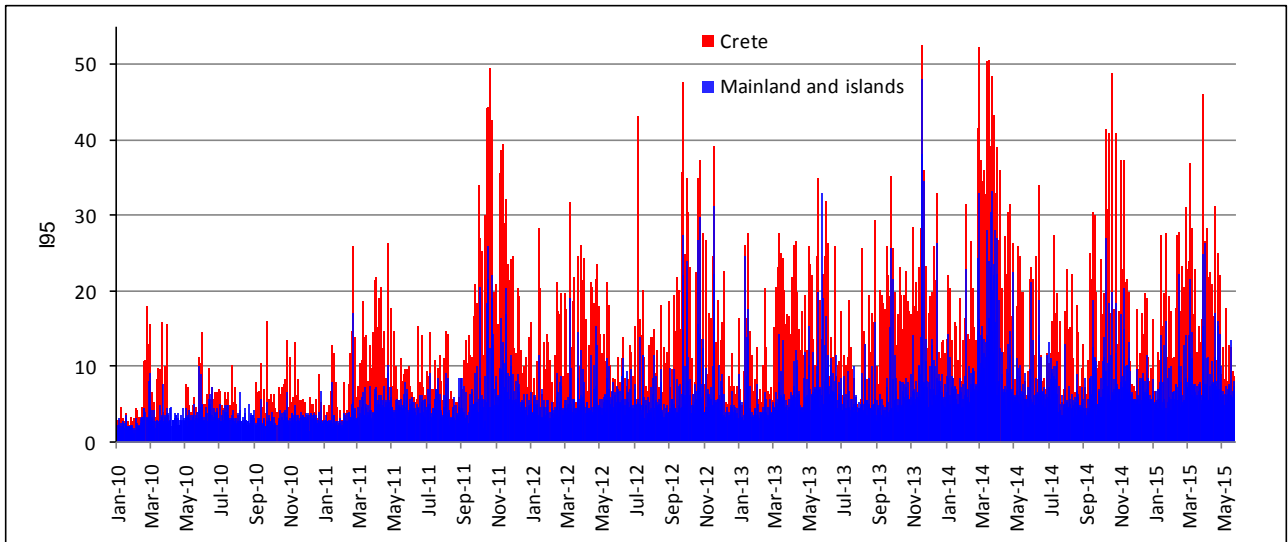


Fig. 1 Maximum daily I95 index estimated from HEPOS.

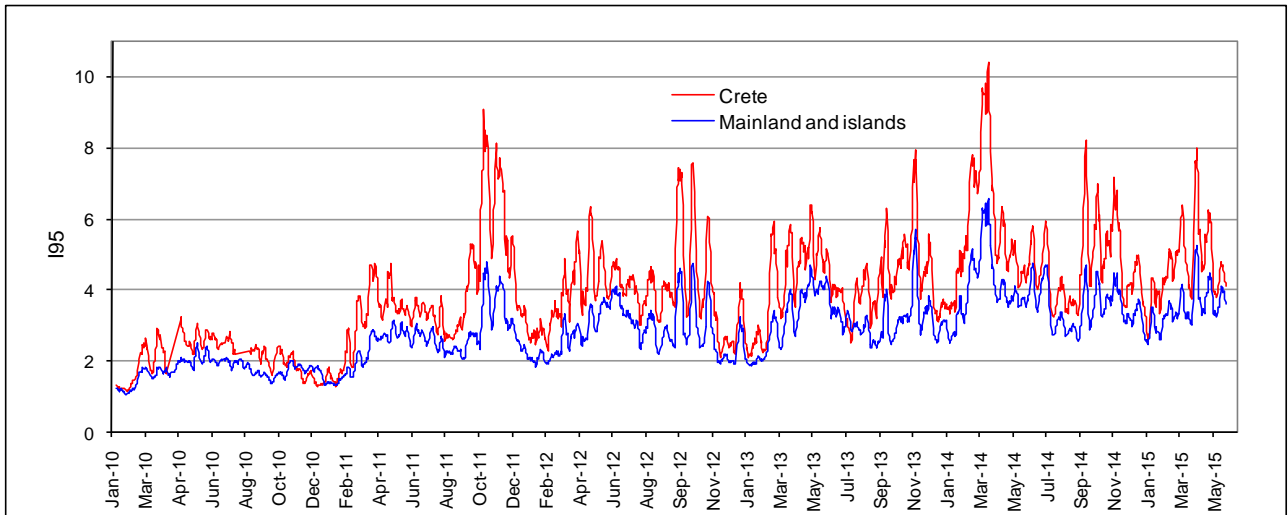


Fig. 2 Mean daily I95 index estimated from HEPOS (values are smoothed using moving average filtering).

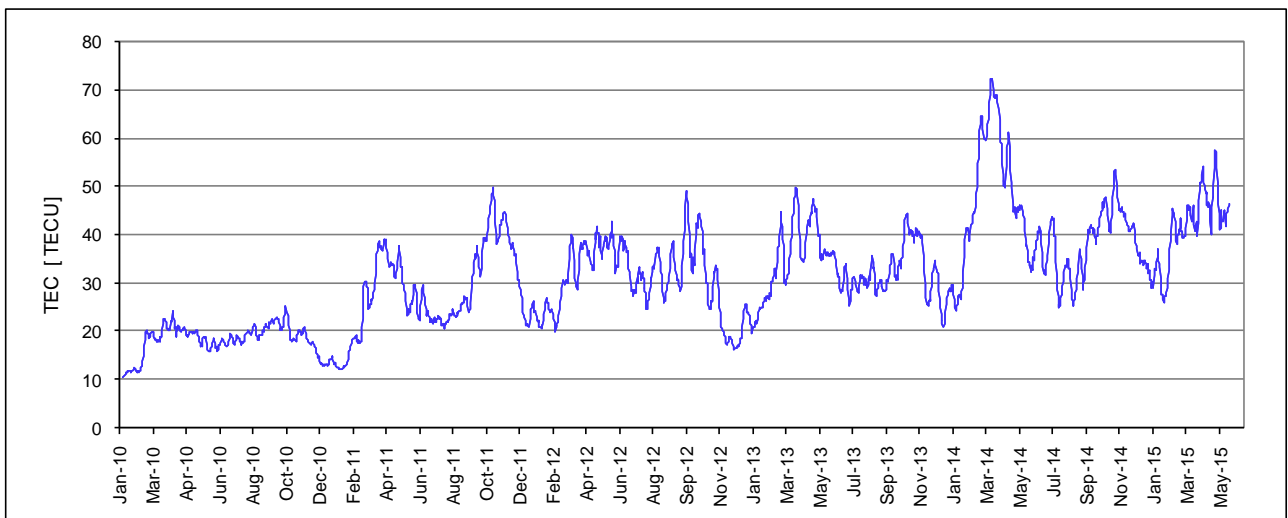


Fig. 3 TEC values for point $\phi=37.5^\circ$, $\lambda= 25^\circ$ at 12:00 UTC obtained from CODE's GIM (values are smoothed using moving average filtering).

ionosphere over a point, whereas the I95 index describes the gradients of the ionospheric delay in the area of an RTK network. Fig. 4 shows the time-series of the sunspot number which clearly indicates that the second peak of the solar activity was higher than the first one.

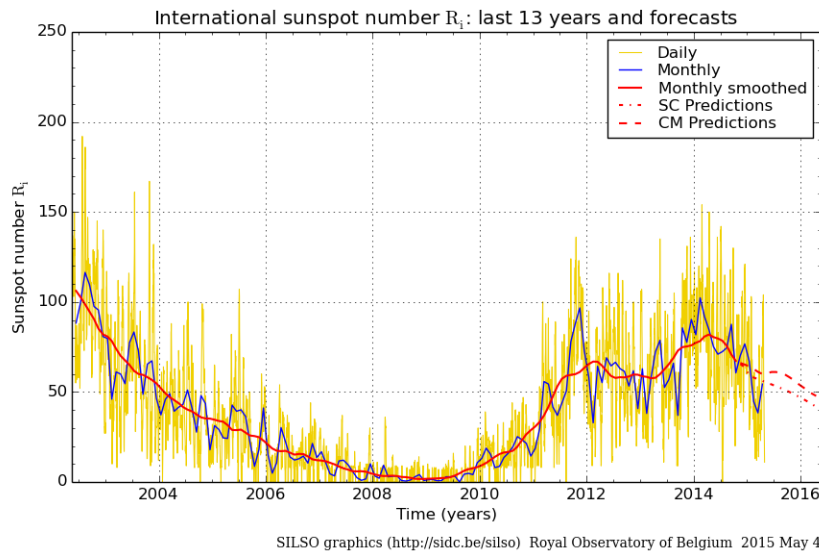


Fig. 4 Sunspot number for the last 13 years (source: Royal Observatory of Belgium)

3. Displacements caused by the 2014 North Aegean Sea earthquake

On 24.5.2014 a strong earthquake ruptured the North Aegean Trough (NAT). The estimated magnitude of the main shock is ranging from $M_w=6.7$ to 6.9 (Saltogianni et al., 2015). Despite its magnitude, the earthquake produced low accelerations even in the vicinity of the epicentral region. Damages were reported mainly at the province of Çanakkale and the surrounding Greek and Turkish islands (Erdik et al., 2014). Significant static horizontal displacements up to 5 cm were reported by *Ganas et al.* (2014) for nearby GNSS stations in Çanakkale and İpsala in Turkey and on

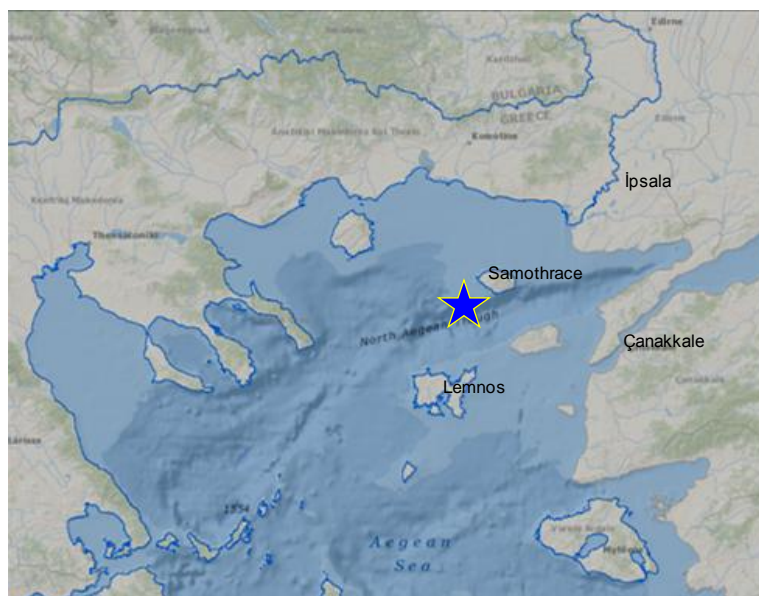


Fig. 5 Epicentre of the May 24, 2014 earthquake (blue star).

Lemnos Island in Greece (Fig. 5). As a first step towards the estimation of the static displacements of HEPOS stations, data from the station 018B on the island of Samothrace were processed. For the processing the Precise Point Positioning (PPP) method (Zumberge et al. 1997; Hérroux and Kouba, 2001) was chosen rather than geodetic relative positioning. This was decided in order to avoid biased displacement estimation as a result of eventual displacements of the nearby stations that would be used as reference in the formation of the baselines. The PPP computations were made using GrafNav ver. 8.40 software. GrafNav computes kinematic baselines and PPP solutions using Kalman filter algorithms and taking advantage of precise orbits, satellites clock errors and DCB (differential code biases) information (Novatel, 2011). Dual frequency phase observations were used together with CODE final precise orbits (sp3 files) and clocks (RINEX clock files) (Kouba, 2003).

3.1 Static displacements

In order to check for static displacements daily RINEX files were processed in static mode using PPP. An interval of 6 weeks (3 weeks before and 3 weeks after the earthquake) was processed. Fig. 6-7 give the time-series of the estimated Easting and Northing coordinates of station 018B. The changes in Easting and Northing are obvious and amount 97 mm and 32 mm, respectively. These coordinate changes correspond to a horizontal displacement of 10.2 cm at an azimuth of 72° as shown in Fig. 8. This result is generally consistent with the morphology of the NAT. The estimated displacement of the station 018B is twice as big as the displacement reported by Ganas et al. (2014) for the station LEMN on Lemnos Island. The difference in the norm of the two displacement vectors can be explained by the fact that Samothrace is much closer to the NAT and to the epicenter of the earthquake than Lemnos (see Fig. 5).

The above mentioned displacement of station 018B exceeds by far any other previously recorded earthquake-induced displacement of a HEPOS station since its start of operation in 2007 (Gianniou, 2011).

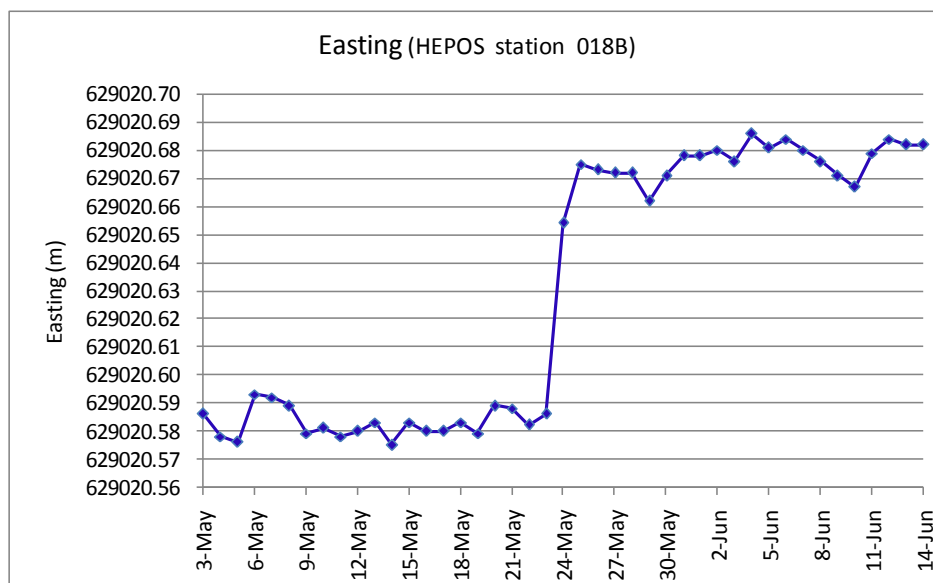


Fig. 6 Time-series of Easting of station 018B.

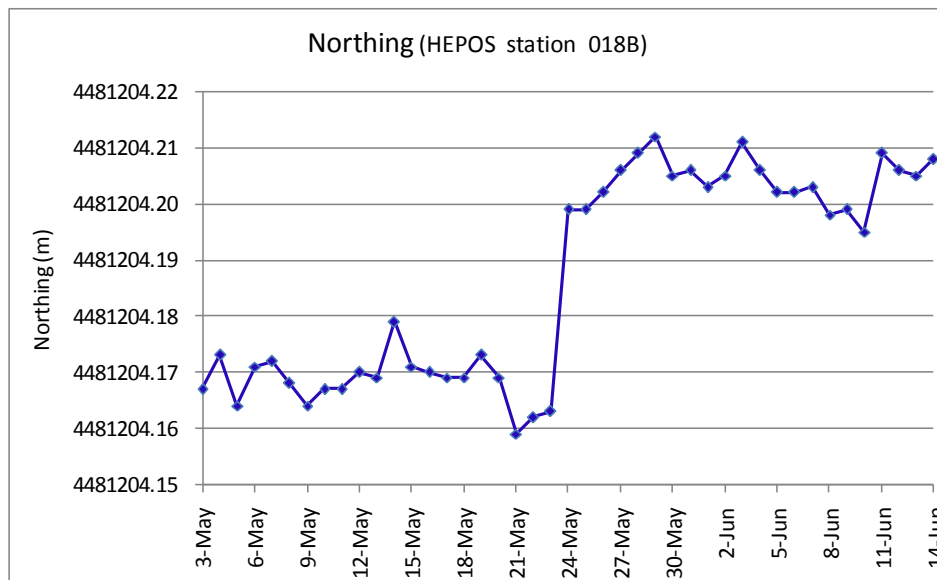


Fig. 7 Time-series of Northing of station 018B.



Fig. 8 Estimated static horizontal displacement of station 018B. The epicentre of the earthquake is marked by blue star.

3.2 Dynamic displacements

In addition to the estimation of static displacements described above, dynamic displacements of station 018B were also estimated. For this purpose 1-Hz data were processed in kinematic mode using PPP. Fig. 9 depicts the resulted variations in the Easting and Northing coordinates of station 018B with respect to mean values of Easting and Northing computed over the time period from 9:24:30 to 9:25:15. Clearly, the earthquake caused a progressive shift to the East that reaches almost 12 cm before it stabilizes to about 9cm. The shift to the North is a bit smaller (almost 8 cm) but it takes place in a much shorter time (7 seconds). Moreover, unlike the shift to the East, most of the northward dynamic displacement is temporal and the station stabilizes to about 3 cm. These apparent final shifts are in good agreement with the estimated static displacement (97 mm to the East and 32 mm to the North) described in section 3.1. A seismological interpretation of the revealed dynamic displacements is beyond the scope of this report, but it could be useful for the

study of the 2014 NAT earthquake, an event characterized by two distinct rupture segments, the second one associated with supershear velocity (Evangelidis, 2014).

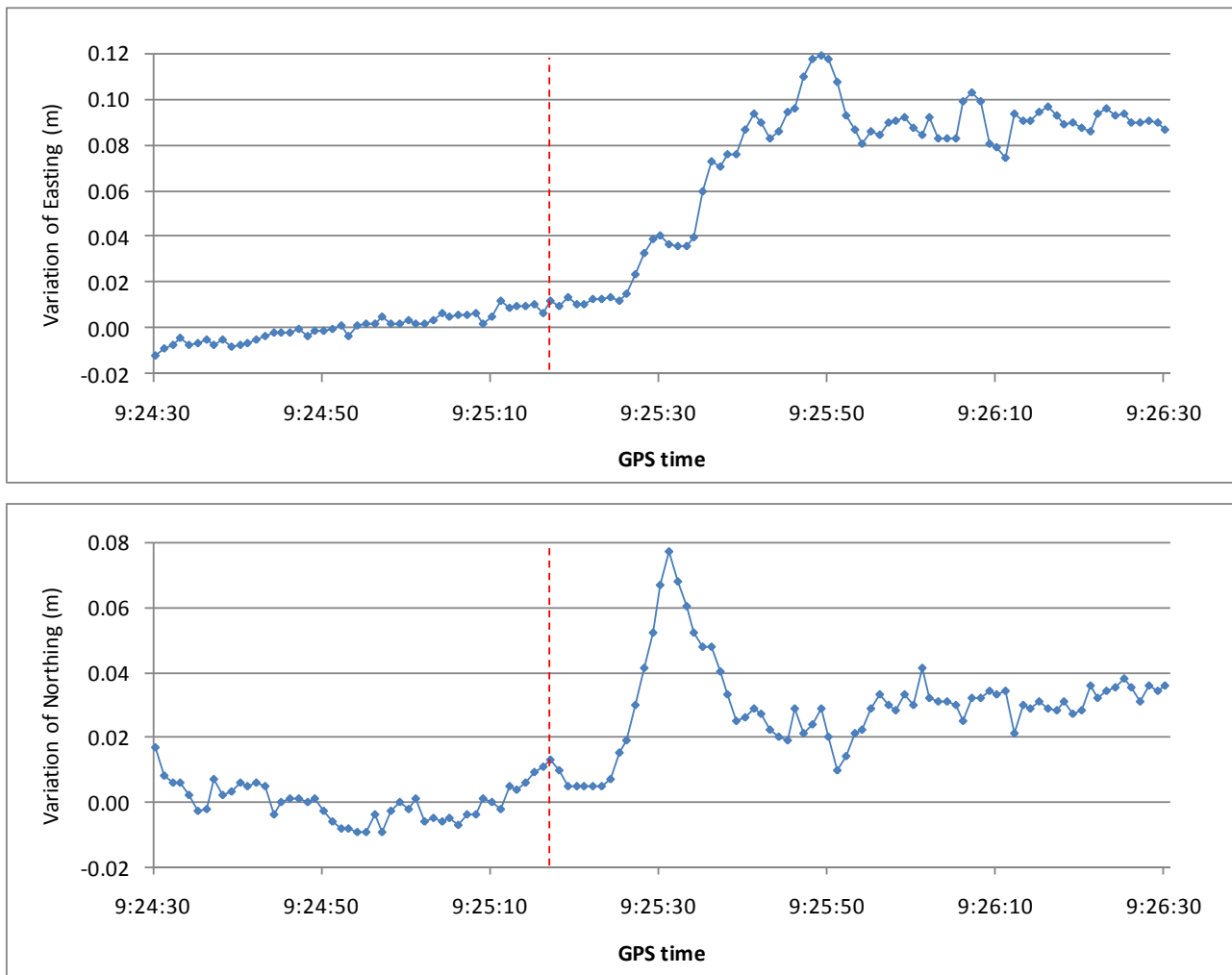


Fig.9 Variations of the coordinates of station 018B shortly before, during and after the earthquake (the vertical dashed line at 09:25:17 GPS time indicates the moment the EQ stroke).

Acknowledgments

The HEPOS project was co-funded by the European Regional Development Fund in the framework of the Operational Program “Information Society”. Mrs. Vasiliki Kalantzi assisted the processing of the ionospheric data.

References

Erdik, M., A. Pnar, S. Akkar, C. Zülfikar, D. Kalafat, K. Kekovali, N. P. Özel, and O. Necmioglu (2014), Earthquake report 24 May 2014 northern Aegean sea, Tech. Rep., Kandilli Observatory and Earthquake Research Institute, Boğaziçi Univ, Istanbul, Turkey.

Evangelidis, C. P. (2014), Imaging supershear rupture for the 2014 Mw 6.9 Northern Aegean earthquake by back projection of strong motion waveforms, *Geophys. Res. Lett.*, 42, 307–315, doi:10.1002/2014GL062513.

Ganas, A., Cannavo, F., Georgiev, I., Kassaras, I., and Moschou, A. (2014), Preliminary GPS results and static stress transfer model for the May 24, 2014 M=6.8 earthquake, North Aegean Sea. Unpublished Web Report, 4 pages, Athens.

Gianniu, M., (2011), Detecting permanent displacements caused by earthquakes using data from the HEPOS network, *EUREF 2011 Symposium*, May 25-28 2011, Chisinau, Moldova.

Gianniu M. and E. Mitropoulou (2012), Impact of high ionospheric activity on GPS surveying: Experiences from the Hellenic RTK-network during 2011-12, *EUREF 2012 Symposium*, June 6-8 2012, Saint Mandé, France.

Gianniu, M., D. Mastoris (2013), National Report of Greece to EUREF 2013, *EUREF 2013 Symposium*, May 29-31 2013, Budapest, Hungary.

Gianniu M., D. Mastoris and E. Mitropoulou (2014), National report of Greece to EUREF 2014, *EUREF 2014 Symposium*, June 3-7 2014, Vilnius, Lithuania.

Héroux, P. and J. Kouba (2001), GPS precise point positioning using IGS orbit products, *Phys. Chem. Earth Part A*, 26(6–8), 573–578, doi:10.1016/S1464-1895(01)00103-X.

Kouba, J. (2003), Measuring seismic waves induced by large earthquakes with GPS. *Stud. Geophys. Geod.* 47(4), 741–755.

Novatel (2011), GrafNav / GrafNet User Guide. http://www.novatel.com/assets/Documents/Waypoint/Downloads/NavNet840_Manual.pdf.

Saltogianni V., M. Gianniu, S. Yolsal-Çevikbilen, T. Eken, T. Taymaz and Stathis Stiros (2015), Seismological and Geodetic Modeling of the 2014, Mw 6.8 Earthquake of North Aegean Trough”, *Geophysical Research Abstracts*, Vol. 17, EGU2015.

Wanninger, L. (1999), The Performance of Virtual Reference Stations in Active Geodetic GPS-Networks under Solar Maximum Conditions. *Proceedings of the 12th International Technical Meeting of the Satellite Division of The Institute of Navigation (ION GPS 99)*, Nashville TN, 1419-1427.

Zumberge, J. F., M. B. Heflin, D. C. Jefferson, M. M. Watkins and F. H. Webb (1997), Precise point positioning for the efficient and robust analysis of GPS data from large networks, *J. Geophys. Res.*, 102(B3), 5005–5017, doi:10.1029/96JB03860.